Synthesis and Characterization of Zinc−Blende CdSe-Based Core/Shell Nanocrystals and Their Luminescence in Water

ARTICLE *in* THE JOURNAL OF PHYSICAL CHEMISTRY C · FEBRUARY 2008

Impact Factor: 4.77 · DOI: 10.1021/jp710648g

4 AUTHORS:

Sung Jun Lim
University of Illinois, Urbana-Champaign
14 PUBLICATIONS **175** CITATIONS
SEE PROFILE

Bonghwan Chon
National Institute of Standards and Technolo…
26 PUBLICATIONS **420** CITATIONS
SEE PROFILE

Taiha Joo
Pohang University of Science and Technology
131 PUBLICATIONS **4,056** CITATIONS
SEE PROFILE

Seung Koo Shin
Pohang University of Science and Technology
79 PUBLICATIONS **1,350** CITATIONS
SEE PROFILE

THE JOURNAL OF PHYSICAL CHEMISTRY C LETTERS

2008, *112,* 1744−1747
Published on Web 01/23/2008

Synthesis and Characterization of Zinc-Blende CdSe-Based Core/Shell Nanocrystals and Their Luminescence in Water

Sung Jun Lim, Bonghwan Chon, Taiha Joo, and Seung Koo Shin*

Bionanotechnology Center, Department of Chemistry, Pohang University of Science and Technology, San 31, Hyoja-Dong, Nam-Gu, Pohang, Kyungbuk, Korea, 790-784

Received: November 6, 2007; In Final Form: January 9, 2008

Zinc-blende CdSe cores are used as a substrate for the synthesis of core/shell nanocrystals, such as CdSe/ZnS, CdSe/ZnSe/ZnS, and CdSe/CdS/ZnS. Only two monolayers of shell coverage for each material suffice to enhance the photoluminescence (PL) quantum efficiency and achieve ∼50% PL efficiency in water from all core/shell nanocrystals after ligand exchange with 3-mercaptopropionic acid. Powder X-ray diffraction (XRD) patterns and high-resolution transmission electron microscopy images confirm the coherent epitaxial growth of the zinc-blende shell for core/shell nanocrystals. The PL spectra obtained at 5 K illustrate the effects of the shell composition on deep-trap emission, which manifests the role of hole-trapping surface defects. The spectral shift in both the first absorption maximum and PL band varies with the shell composition following the simple band-offset picture. The shell-to-shell variation of the spectral shift and changes in XRD patterns suggests that the contraction of CdSe lattice occurs with the concomitant redshift in the PL band, most notably with the ZnS shell. Water-soluble nanocrystals show longer PL lifetimes than organic-soluble ones. The zinc-blende structure is considered a viable alternate replacing the wurtzite structure for the uniform growth of shells and the isotropic incorporation of capping ligands.

Semiconductor nanocrystals have shown great promise as a new class of fluorophores in biological imaging.[1−3] They offer high photostability, size-tunable emission with narrow bandwidth, and broad excitation wavelength.[1−3] Thus, nanocrystal fluorophores have attracted much interest on expectation of highly sensitive multiple color detection of biomolecules with a single light source.[1−3] Among various semiconductor materials, CdSe has been most extensively studied because their size-tunable emission lies in the visible region.[4−6] They are typically synthesized in organic solvent at high temperature and then converted into water-soluble forms for conjugation with biomolecules.[2,3] However, CdSe nanocrystals often lose luminescence after water-soluble ligand exchange due to the leakage of exciton into the surrounding. Larger band gap materials, such as ZnS,[6−8] CdS,[8−11] and ZnSe,[8,12] or their alloys,[13] have been employed to suppress the exciton leakage by forming the core/shell structure. Although the core/shell composite greatly enhances photoluminescence (PL), the quantum efficiency (QE) varies nonlinearly with shell thickness: QE rises sharply in the beginning, reaches the top, and then declines. In the case of wurtzite (W) CdSe-based core/shell nanocrystals, QE reaches the maximum of ∼50% with a 1.3 monolayer (ML) thick ZnS shell,[7] ∼80% with 2 ML thick ZnSe shell,[8] and ∼60−70% with a 2−3 ML thick CdS shell[9,10] and then declines gradually with increasing shell thickness due to growing surface defects.

Recently, CdSe-based core/shell nanocrystals have been introduced in Förster resonance energy transfer (FRET) as a donor fluorophore, however, their shell thickness really matters now because the efficiency of FRET is extremely sensitive to the distance between the donor and acceptor fluorophores.[3] For the most effective biological FRET imaging, the donor fluorophore needs to be as small and bright as possible in water. To date, most water-soluble nanocrystal fluorophores have been based on W CdSe/ZnS nanocrystals. Unfortunately, their QEs drop significantly from 50−70% in organic solvent to below 10−20% after water-soluble ligand exchange.[6−8,14] A more elaborate core/shell structure has yielded 48% QE in water but with a thick shell.[13] Thus, a key to the success lies on how to grow shells uniformly with the least amount of materials, but without losing luminescence in water. In this work, we present zinc-blende (ZB) CdSe-based core/shell nanocrystals with only 2 MLs of CdS, ZnSe, and/or ZnS shells, which result in nearly 50% QEs in water after capping with 3-mercaptopropionic acid (MPA).

We choose the ZB structure because it is a natural alternate replacing the W structure. Besides, there have been no reports of ZB CdSe-based core/shell nanocrystals and their PL properties in water. W CdSe-based core/shell nanocrystals are reported to have a highly anisotropic and nonuniform shell distribution.[15] Yu et al.[15] have suggested that the different chemical reactivity of dissimilar crystal faces on the W CdSe core leads to the anisotropic and nonuniform shell distribution. Erwin et al.[16] have found that the manganese doping on CdS, ZnSe, and CdSe nanocrystals is highly facet dependent, and the ZB structure incorporates dopants more easily than the W structure. It appears that the shell growth over the W CdSe core is kinetically driven along the *c*-axis,[8] consequently bearing an anisotropic and nonuniform distribution of shell materials. By contrast, the ZB

* Corresponding author. E-mail: skshin@postech.ac.kr.

10.1021/jp710648g CCC: $40.75

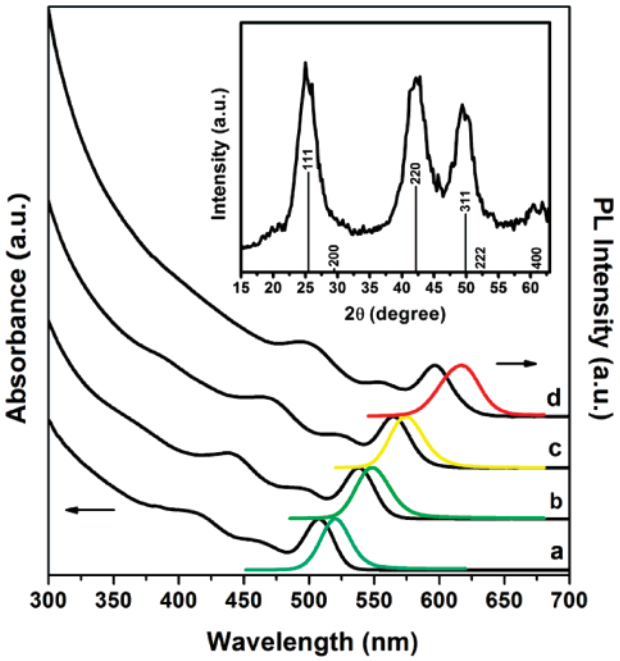

Figure 1. Absorption (black) and emission (color) spectra of CdSe nanocrystals obtained from four separate 2 mmol reactions. For each color, the growth temperature *T* (°C), the time duration (min) to reach *T* from 150 °C, and the dwell time (min) at *T* are (a) 220, 3, 0; (b) 240, 4, 0; (c) 240, 4, 10; and (d) 240, 4, 35, respectively. The emission maximum (nm) and bandwidth (nm) are (a) 520, 23; (b) 547, 23; (c) 573, 25; and (d) 614, 28, respectively. The inset shows the XRD pattern of the sample (b). The vertical lines represent the diffraction patterns for bulk ZB CdSe.

structure has a more isotropic distribution of facets, which could incorporate shell materials more isotropically and lead to a more uniform shell distribution with less surface defects. To test this idea, we prepared ZB CdSe/ZnS, CdSe/ZnSe/ZnS, and CdSe/CdS/ZnS nanocrystals as well as MPA-capped water-soluble nanocrystals. Herein we report synthetic methods, X-ray diffraction (XRD) patterns, high-resolution transmission electron microscopy (HRTEM) images, the optical spectra in solution, and the PL spectra at 5 K, as well as the PL efficiencies with lifetimes.

ZB CdSe nanocrystals were synthesized by following a noninjection scheme,[17] but cadmium stearate was used in place of cadmium myristate. The reaction becomes less sensitive to the purity of cadmium precursor. Moreover, there is no need for oleic acid during the growth. Figure 1 shows the optical spectra of CdSe nanocrystals and the XRD pattern of the sample b. The wide gap between the first ($1S_{3/2}1S_e$) and second ($2S_{3/2}1S_e$) exciton absorption peaks is the typical feature of ZB CdSe nanocrystals.[17−19] The XRD pattern also shows the highly crystalline ZB structure: the deep valley between (220) and (311) peaks, and the appreciable (400) peak, which is absent in the W structure.[17]

All core/shell nanocrystals were synthesized from the same ZB CdSe core by adopting both dropwise[7] and successive ion layer adsorption reaction[11] methods. Each shell was grown layer-by-layer over the core up to 2 MLs. Figure 2 displays the XRD patterns from all core/shell nanocrystals. All of them show bulk ZB patterns, suggesting that the epitaxial growth of shell carries the ZB phase of the core to the shell. In the case of CdSe/ZnS nanocrystals, the ZnS shell grows with the bulk lattice parameter at the coverage of 2 MLs, while 4 MLs of ZnS coverage induces a sharper (220) reflection, revealing a tendency of shell growth toward a [220] direction perpendicular to the *c*-axis. On the

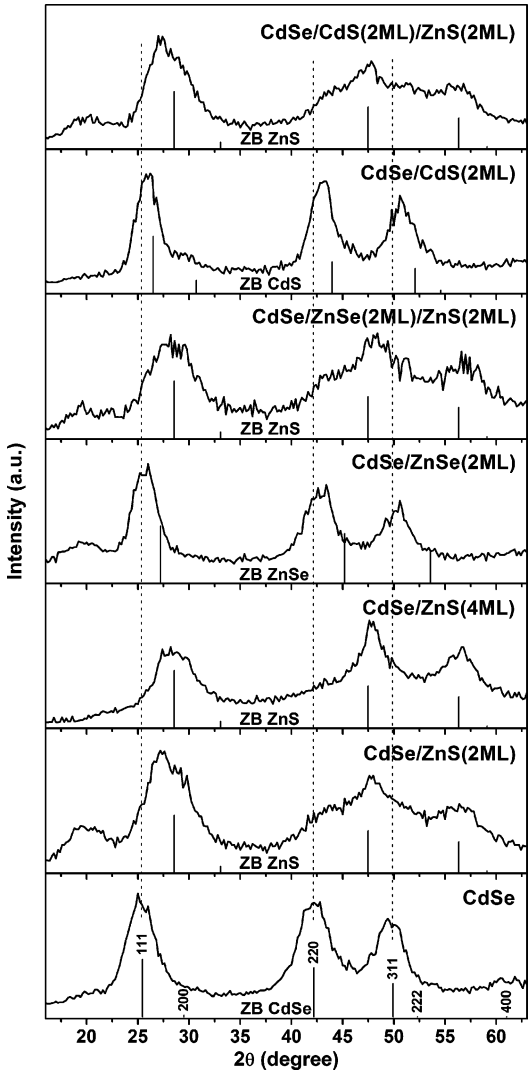

Figure 2. XRD patterns of core/shell nanocrystals synthesized from the same 2.7 nm ZB CdSe nanocrystals (the sample of Figure 1b). Vertical lines represent the diffraction patterns for bulk ZB compounds. The shell thickness is denoted in parenthesis in units of monolayer.

other hand, both ZnSe(2ML) and CdS(2ML) shells induce little changes from the CdSe pattern, suggesting the coherent epitaxial growth of the shell over the core with the expansion of shell lattice. In CdSe/ZnSe/ZnS and CdSe/CdS/ZnS nanocrystals, the outermost ZnS shell grows like bulk. Apparently, the growth of the outermost ZnS shell with the bulk lattice parameter induces the contraction of underneath layers to accommodate the core−shell lattice mismatch.[20] HRTEM images of all core/shell nanocrystals are shown in Figure S1 (see Supporting Information). Nanocrystals appear mostly spherical with an incremental increase of nanocrystal size expected from the shell growth but without any odd defect or significant anisotropic morphology. These HRTEM images also illustrate the epitaxial shell growth over the ZB core.

Figure 3a−c shows the shell-to-shell variation of the optical spectra and QEs. Both the first excition absorption peak and emission band shift to red with increasing shell thickness, which ensures the formation of a core/shell composite rather than an alloy.[13] The purified ZB CdSe nanocrystals yield only 4% QE; however, the successive growth of 2 MLs of shell drastically increases QE to 71 and 77% in CdSe/ZnS and CdSe/ZnS/ZnS, 19 and 82% in CdSe/ZnSe and CdSe/ZnSe/ZnS, and 29 and 56% in CdSe/CdS and CdSe/CdS/ZnS, respectively. In contrast,

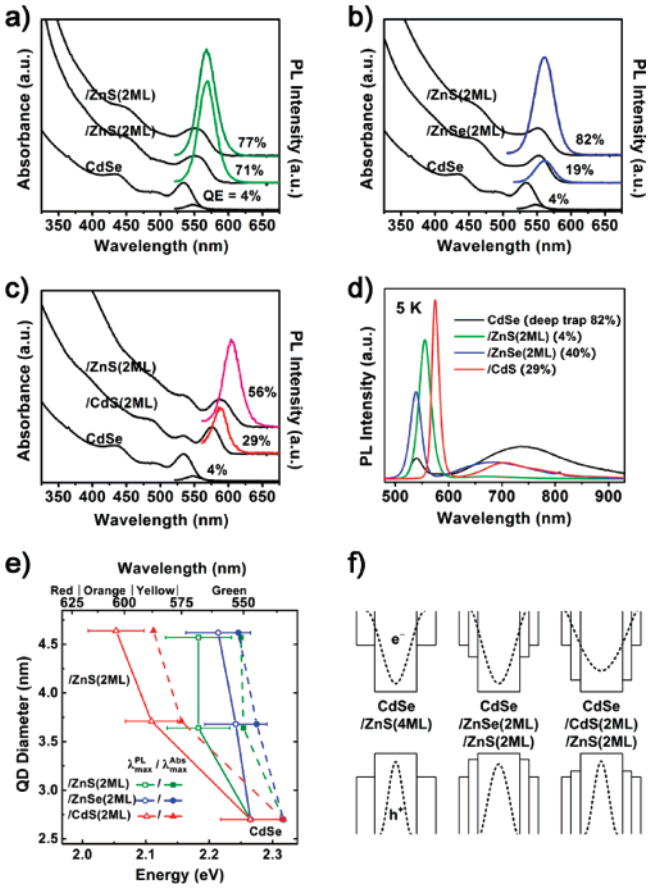

Figure 3. Absorption and emission spectra of organic-soluble nanocrystals: (a) CdSe/ZnS, (b) CdSe/ZnSe/ZnS, and (c) CdSe/CdS/ZnS nanocrystals dissolved in chloroform. QE is measured relative to Rhodamine B in methanol (85% QE). (d) The PL spectra of nanocrystals at 5 K. The percentage of deep trap emission is given in parentheses. e) The shell-to-shell variation of the first exciton absorption peak (solid symbols), the emission maximum (open symbols), and the size of nanocrystals. Error bars represent emission bandwidths (full width at half-maximum). (f) A simplified band-offset picture for the core/shell structure. Dotted lines illustrate wavefunctions for electron and hole.

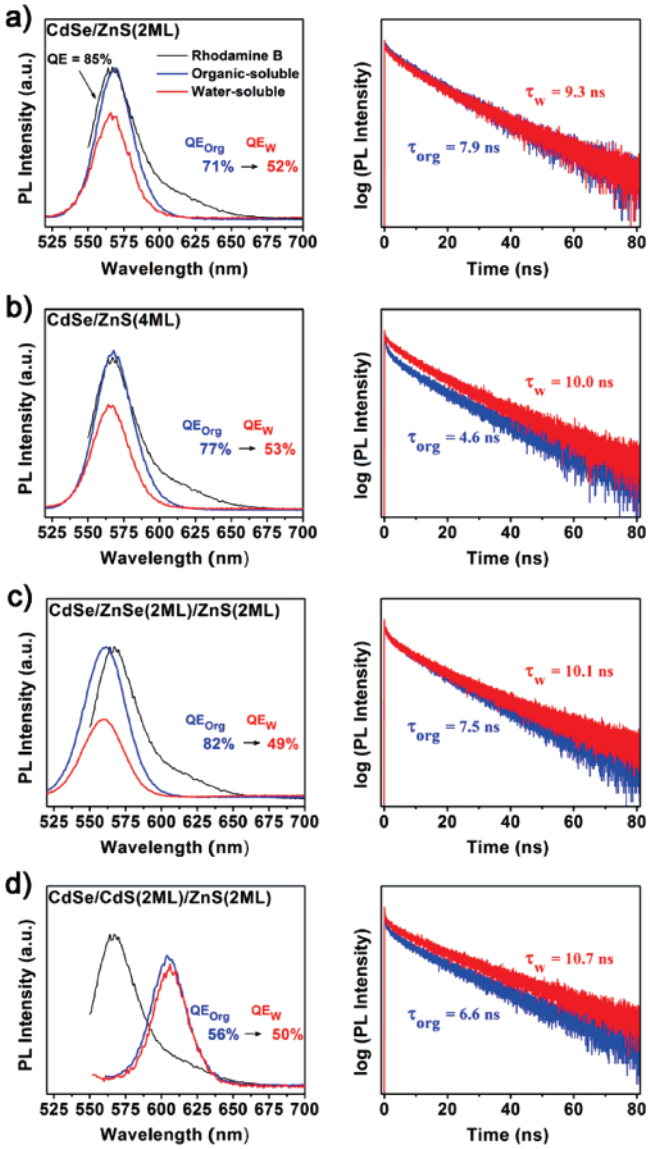

Figure 4. PL spectra and time-resolved PL decay of organic-soluble (blue) and MPA-capped water-soluble (red) nanocrystals dissolved in either chloroform or water. The laser fluence used in PL decay measurement is ~2.5 μJ cm^{-2}.

QEs of most W CdSe-based nanocrystals diminish after 1−2 MLs of shell.[6−8] Continual increase of QE with increasing shell thickness manifest the coherent epitaxial growth of shells over the ZB CdSe core.

The effects of the core/shell structure on deep trap emission (DTE) were examined by taking the PL spectra of nanocrystals at 5 K. Figure 3d reveals the amount of DTE from the core/shell structure (see Figure S2 in Supporting Information). The purified ZB CdSe cores exhibit strong DTE with an 82% population. The 2 MLs of ZnS shell greatly reduce DTE to 4%; however, an additional 2 MLs of ZnS shell increase DTE to 6%, suggesting that 4 MLs of ZnS shell is beyond the limit of coherent epitaxial growth. On the other hand, 2 MLs of ZnSe and CdS shells reduce DTE to 40 and 29%, respectively. Apparently, hole-traps contribute more to DTE than electron traps. Meanwhile, additional 2 MLs of ZnS shell over ZnSe and CdS shells suppress DTE to 4 and 2%, respectively. This great suppression of DTE and the epitaxial lattice structure shown in Figure 2 provide further evidence for the coherent epitaxial growth of shells over the ZB cores in CdSe/ZnSe/ZnS and CdSe/CdS/ZnS nanocrystals. Figure 3e depicts the optical properties and the size of nanocrystals as a function of core/shell structure. Figure 3f illustrates the simple band-offset picture for comparison of the band structure: The ZnS shell setting up potential barriers for both electron and hole effectively suppresses the exciton leakage (77% QE), the ZnSe shell expanding the valence band leads to a better exciton overlap (82% QE), while the CdS shell expanding the conduction band efficiently lowers the band gap but reduces the exciton overlap (56% QE). The outermost ZnS shell induces 0, 7, and 16 nm red shift in CdSe/ZnS (4ML), CdSe/ZnSe/ZnS, and CdSe/CdS/ZnS nanocrystals, respectively. Interestingly, the redshift of emission occurs when the outermost ZnS shell induces the contraction of CdSe lattice, which destabilizes both electron and hole energy levels to give a lower band gap.

Finally, we made core/shell nanocrystals water-soluble by capping with MPA. Figure 4 shows the emission spectra, PL efficiency, and time-resolved PL decay. After water-soluble ligand capping, QE decreases to 52, 53, 49, and 50% for CdSe/ZnS (2ML), CdSe/ZnS (4ML), CdSe/ZnSe/ZnS, CdSe/CdS/ZnS nanocrystals, respectively. In contrast, W CdSe/ZnS nanocrystals with 1−2 MLs of shell coverage often do not luminesce in water.[3] Even with a thick (5−7 MLs) ZnS shell, they show only 10−20% QEs.[14] Achieving nearly 50% QE in water from all ZB core/shell nanocrystals with only 2 MLs of coverage for

each shell is quite remarkable. Because MPA quenches luminescence when directly bound to the bare CdSe core,[21] these high QEs suggest the absence of the bare CdSe surface directly exposed to MPA in water, implying that the shell grows uniformly over the ZB core with a lesser amount of materials than the W core. To gain insights into the exciton recombination dynamics, we studied the time-resolved PL decay in solution. The PL lifetimes (τ_{org}, τ_w in ns) for organic and water-soluble nanocrystals are (7.9, 9.3), (4.6, 10.0), (7.5, 10.1), and (6.6, 10.7) for CdSe/ZnS (2ML), CdSe/ZnS (4ML), CdSe/ZnSe/ZnS, and CdSe/CdS/ZnS, respectively (see Table S2 in Supporting Information for the fitting parameters). In general, water-soluble nanocrystals exhibit longer lifetimes than organic-soluble ones. The most notable changes occur in going from CdSe/ZnS (2ML) to CdSe/ZnS (4ML), a decrease in lifetime from 7.9 to 4.6 ns in chloroform and an increase from 9.3 to 10.0 ns in water. For all samples, the CdSe core is from the same batch, and the outermost shell is composed of the same material and also covered with the same capping ligand (1-dodecylamine and MPA in organic and water-soluble nanocrystals, respectively) under the same environment. Thus, shell-to-shell variations of the three-component PL decay may be due to dissimilar core/shell band structures, interfacial defects, and/or intrinsic states of the CdSe core as suggested by Morello et al.[22] The lifetime elongation in water may be due to the coordination of MPA to the surface Zn atom, which removes potential electron traps on the outermost surface of nanocrystals.[23] Besides, the femtosecond laser pulse employed in our experiment may have complicated the exciton dynamics by generating more than a single exciton. Further investigations are warranted to gain a better understanding of the exciton dynamics.

In conclusion, the zinc-blende structure is better than the wurtzite structure in growing shells more uniformly. We demonstrate the uniform and coherent epitaxial growth of double shells over zinc-blende CdSe nanocrystals with only two monolayers of shell thickness for both inner and outer shells. This uniform and coherent shell growth with an isotropic ligand capping allows retaining high quantum efficiencies in water-soluble nanocrystals.

Acknowledgment. We thank Mr. Y. K. Kim and National Center for Nanomaterials and Technology for taking HRTEM images. We acknowledge supports from POSTECH Biotech Center, NT−BT Measurement and Manipulation Project, Advanced Scientific Analysis Instruments Development Project (Grant RH0-2005-000-01004-0), Korea Research Foundation (Grant KRF-2004-005-C00004, KRF-2006-005-J01202), and Korea Foundation for International Cooperation of Science and Technology (K20501000002-07-E0100-00210). We also thank the Pohang Acceleratory Laboratory for the XRD measurement.

Supporting Information Available: Syntheses, experimental procedures for the PL measurements and HRTEM imaging, HRTEM images, the PL spectra at 5 K, the size and optical properties of nanocrystals, and the relative strengths of the three PL decay components. This material is available free of charge via the Internet at http://pubs.acs.org.

References and Notes

(1) Shin, S. K.; Yoon, H. -J.; Jung, Y. J.; Park, J. W. *Curr. Opin. Chem. Biol.* **2006**, *10*, 423.
(2) Michalet, X.; Pinaud, F. F.; Bentolila, L. A.; Tsay, J. M.; Doose, S.; Li, J. J.; Sundaresan, G.; Wu, A. M.; Gambhir, S. S.; Weiss, S. *Science* **2005**, *307*, 538.
(3) Medintz, I. L.; Uyeda, H. T.; Goldman, E. R.; Mattoussi, H. *Nat. Mater.* **2005**, *4*, 435.
(4) Murray, C. B.; Norris, D. J.; Bawendi, M. G. *J. Am. Chem. Soc.* **1993**, *115*, 8706.
(5) Qu, L.; Peng, Z. A.; Peng, X. *Nano Lett.* **2001**, *1*, 333.
(6) Talapin, D. V.; Rogach, A. L.; Kornowski, A.; Hasse, M.; Weller, H. *Nano Lett.* **2001**, *1*, 207.
(7) Dabbousi, B. O.; Rodriguez-Viejo, J.; Mikulec, F. V.; Heine, J. R.; Mattoussi, H.; Ober, R.; Jensen, K. F.; Bawendi, M. G. *J. Phys. Chem. B* **1997**, *101*, 9463.
(8) Talapin, D. V.; Mekis, I.; Götzinger, S.; Kornowski, A.; Benson, O.; Weller, H. *J. Phys. Chem. B* **2004**, *108*, 18826.
(9) Peng, X.; Schlamp, M. C.; Kadavanich, A. V.; Alivisatos, A. P. *J. Am. Chem. Soc.* **1997**, *119*, 7019.
(10) Mekis, I.; Talapin, D. V.; Kornowski, A.; Haase, M.; Weller, H. *J. Phys. Chem. B* **2003**, *107*, 7454.
(11) Li, J. J.; Wang, Y. A.; Guo, W.; Keay, J. C.; Mishima, T. D.; Johanson, M. B.; Peng, X. *J. Am. Chem. Soc.* **2003**, *125*, 12567.
(12) Reiss, P.; Bleuse, J.; Pron, A. *Nano Lett.* **2002**, *2*, 781.
(13) Xie, R.; Kolb, U.; Li, J.; Basché, T.; Mews, A. *J. Am. Chem. Soc.* **2005**, *127*, 7480.
(14) Mattoussi, H.; Mauro, J. M.; Goldman, E. R.; Anderson, G. P.; Sundar, V. C.; Mikulec, F. V.; Bawendi, M. G. *J. Am. Chem. Soc.* **2000**, *122*, 12142.
(15) Yu, Z.; Guo, L.; Du, H.; Krauss, T.; Silcox, J. *Nano Lett.* **2005**, *5*, 565.
(16) Erwin, S. C.; Zu, L.; Haftel, M. I.; Efros, A. L.; Kennedy, T. A.; Norris, D. J. *Nature* **2005**, *436*, 91.
(17) Yang, Y. A.; Wu, H.; Williams, K. R.; Cao, Y. C. *Angew. Chem. Int. Ed.* **2005**, *44*, 6712.
(18) Mohamed, M. B.; Tonti, D.; Al-Salman, A.; Chemseddine, A.; Chergui, M. *J. Phys. Chem. B* **2005**, *109*, 10533.
(19) Jasieniak, J.; Bullen, C.; van Embden, J.; Mulvaney, P. *J. Phys. Chem. B* **2005**, *109*, 20665.
(20) Yun, S. J.; Lee, G.; Kim, J. S.; Shin, S. K.; Yoon, Y.-G. *Solid State Commun.* **2006**, *137*, 332.
(21) Wuister, S. F.; de Mello Donega, C.; Meijerink, A. *J. Phys. Chem. B* **2004**, *108*, 17393.
(22) Morello, G.; Anni, M.; Cozzoli, P. D.; Manna, L.; Cingolani, R.; De Giorgi, M. *J. Phys. Chem. C* **2007**, *111*, 10541.
(23) Jeong, S; Achermann, M.; Nanda, J.; Ivanov, S.; Klimov, V. I.; Hollingsworth, J. A. *J. Am. Chem. Soc.* **2005**, *127*, 10126.